Large area event counting detectors with high spatial and temporal resolution

2014 JINST 9 C04002

(http://iopscience.iop.org/1748-0221/9/04/C04002)

Jinst
PUBLISHED BY IOP PUBLISHING FOR SISSA MEDIALAB
RECEIVED: *December 13, 2013*
ACCEPTED: *February 11, 2014*
PUBLISHED: *April 2, 2014*

15th INTERNATIONAL WORKSHOP ON RADIATION IMAGING DETECTORS
23–27 JUNE 2013,
PARIS, FRANCE

Large area event counting detectors with high spatial and temporal resolution

O.H.W. Siegmund,[a,1] **J.B. McPhate,**[a] **J.V. Vallerga,**[a] **A.S. Tremsin,**[a] **H.E. Frisch,**[b] **J.W. Elam,**[c] **A.U. Mane**[c] **and R.G. Wagner**[c]

[a]*Space Sciences Laboratory, University of California at Berkeley, Berkeley, CA 94720, U.S.A.*
[b]*Enrico Fermi Institute, University of Chicago, Chicago, Il 60637, U.S.A.*
[c]*Argonne National Laboratory, Lemont, Il 60439, U.S.A.*

E-mail: ossy@ssl.berkeley.edu

ABSTRACT: Novel large area microchannel plates (MCPs) constructed using micro-capillary arrays functionalized by atomic layer deposition (ALD) have been successfully demonstrated in large format detectors (10 cm and 20 cm) with cross delay line and cross strip readouts. Borosilicate micro-capillary substrates allow robust MCPs to be made in sizes to 20 cm, the intrinsic background rates are low (< 0.06 events cm^{-2} sec^{-1}), the channel open area can be made as high as 85%, and the gain after preconditioning (vacuum bake and burn-in) shows virtually no change over > 7 C cm^{-2} extracted charge.

We have constructed a number of detectors with these novel MCPs, including a 10×10 cm cross strip readout device and 20×20 cm delay line readout sensors. The cross strip detector has very high spatial resolution (the 20 μm MCP pores can be resolved, thus obtaining $\sim$ 5k $\times$ 5k resolution elements), good time resolution (< 1 ns), and high event rate (> 5 million counts/s at 20% dead time), while operating at relatively low gain ($\sim 10^6$). The 20×20 cm delay line detectors have achieved spatial resolutions of $\sim 50\,\mu$m and event rates of several MHz, with good gain and background uniformity and < 200 ps event time tagging. Progress has also been made in construction of a 20×20 cm sealed tube optical imager, and we have achieved > 20% quantum efficiency and good uniformity for large area (20 cm) bialkali photocathodes.

KEYWORDS: Cherenkov detectors; Photon detectors for UV, visible and IR photons (vacuum); Detectors for UV, visible and IR photons; Space instrumentation

[1]Corresponding author.

doi:10.1088/1748-0221/9/04/C04002

2014 JINST 9 C04002

Contents

1 Introduction

Microchannel plate (MCP) detector systems [1] offer a unique set of implementation and performance characteristics that match well with applications requiring event counting, with imaging and timing information. Standard glass based MCPs [2] have been used for decades as a fundamental element in many sensors. MCP based sensors can provide spatial resolutions of less than 10 μm, timing information down to the 10 ps level, formats up to $\sim$ 100 mm and event rates up to 10's of MHz. However, little has changed in their standard production methodology and performance characteristics for many years. Very recently however, fabrication of MCPs using borosilicate glass micro-capillary arrays [3] functionalized by atomic layer deposition (ALD) [4] has been accomplished. The micro-capillary array fabrication closely follows the process for standard glass MCPs [2] except that the substrate is made using hollow borosilicate tubes, and no etching of core glasses is needed. Deposition of a resistive layer and then a secondary emissive layer by ALD produces a functional MCP, eliminating many of the steps used for fabricating standard MCPs. Many of the performance characteristics are similar to conventional MCPs [1], however there are several properties that make them uniquely useful. Some of the most important changes are the ability to make robust MCPs in sizes up to 20 cm with intrinsically low background rates, high gain, high open area ratios, good gain stability and low outgassing rates. We have investigated ALD MCPs applied to large area detector devices and report on their current status.

2 20 cm and 10 cm detector systems with ALD microchannel plates

We have constructed several large detector devices using ALD borosilicate substrate MCPs. In 20 cm format we have developed an open face device [5] with a cross delay line readout for high resolution imaging, and have also been implementing a sealed tube 20 cm format device with stripline readout (figure 2) [5]. In 10 cm format we have developed an open face detector with a cross strip readout for very high spatial resolution and counting rates (figure 3). The 20 cm detectors were

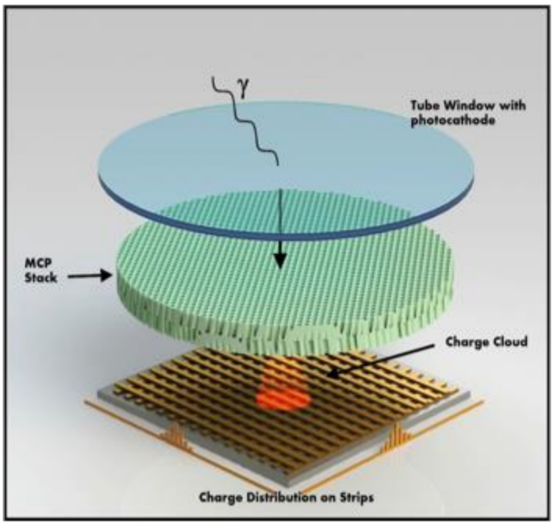

Figure 1. Schematic representation of a sealed tube sensor with a cross strip readout anode and microchannel plates.

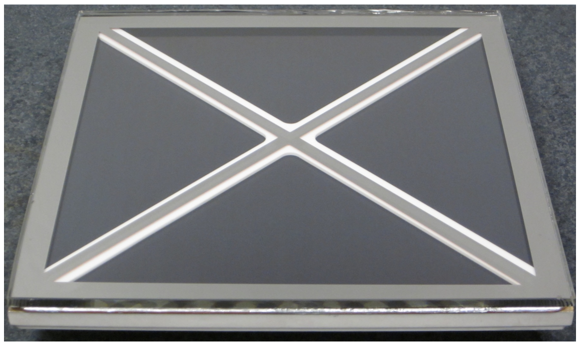

Figure 2. 20×20 cm sealed tube test detector with an ALD MCP pair, bialkali cathode and stripline readout.

developed under the auspices of the Large Area Picosecond PhotoDetector (LAPPD) collaboration [4] with the aim of implementing a 20 cm sealed tube detector with < 10 ps time resolution for High Energy Physics and other applications. The open face 20 cm detector has been used for evaluation of the borosilicate substrate, ALD 20 cm MCPs and provides high spatial resolution ($< 100\,\mu$m) imaging capability at MHz counting rates using a cross delay line photon counting readout [6]. The 20 cm sealed tube detector has a 34 conductive strip readout where the ends of each strip are brought outside the sealed tube package with hermetic pin feedthroughs [5]. For the purposes of testing of these devices we have connected the adjacent strips together to form a continuous serpentine delay line. We then used our delay line electronics encoding systems to determine both X and Y positions of individual events from the differences in the arrival times (~ 100 ns total end to end delay time) at the ends of this anode scheme to give relatively coarse image resolution ($\sim 34 \times 50$ pixels).

The 95 mm cross strip detector (figure 3) was developed for very high spatial resolution ($< 25\,\mu$m) and counting rates (5 MHz) for applications in space astrophysics. It has an 128×128 orthogonal strip readout multilayer anode (figure 4) [7] which detects the charge clouds from an MCP pair (figure 1) and determines the centroid in space and time for each event. The anode signals are sensed by parallel multichannel ASIC preamplifiers (preshape-32, 40 ns peaking time [7]) with output buffering, mounted externally to the detector anode vacuum flange (figure 5). These signals are transferred to a signal processing electronics box (figure 6) set containing a full set of 55 MHz ADCs for digitizing each amplifier channel and a Virtex 6 FPGA to perform the algorithms for event position and time centroiding. These electronics determine the position centroid from the distribution of charge on the anode strips and the time from the digitized time sequence of the charge pulse development. On the 95 mm readout format the position result is digitized to the equivalent of a $6\,\mu$m position bin sampling and the timing is interpolated to ~ 2 ns. Test results show that we achieve an event rate throughput of $\sim 80\%$ at 5 MHz input event rates.

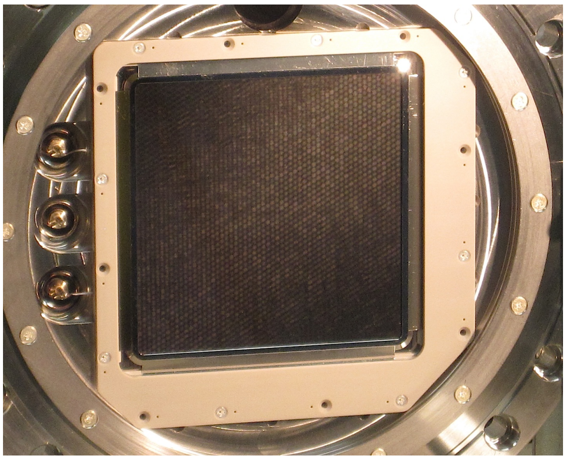

Figure 3. 95 mm cross strip readout detector with a 20 μm pore, 60 : 1 L/D, atomic layer deposited, borosilicate MCP pair.

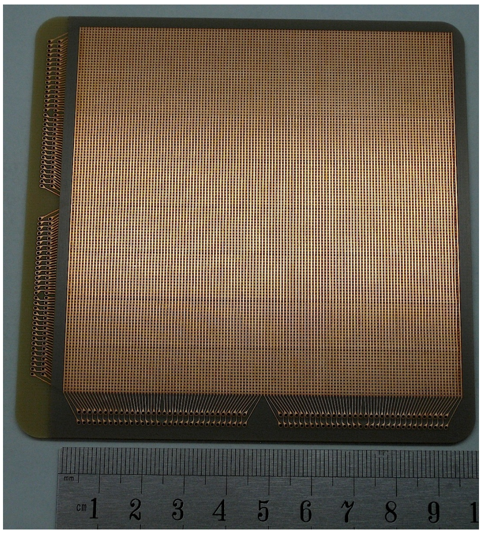

Figure 4. 95 mm cross strip anode design with 128 $\times$ 128 strips for charge signal collection & location.

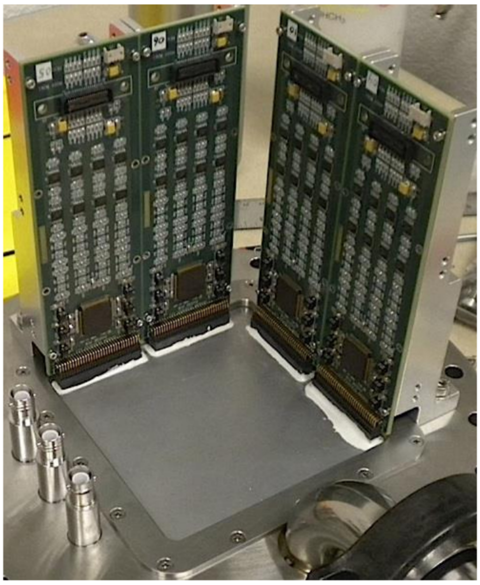

Figure 5. 95 mm cross strip detector showing the 4 $\times$ 64 channel amplifiers connected to the anode.

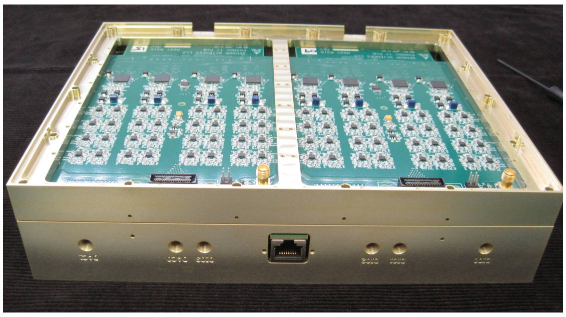

Figure 6. Parallel cross strip electronics signal processing boards with 128 channel ADCs and FPGA encoder.

3 Atomic layer deposited microchannel plate performance

Considerable work has been done in the development of ALD microchannel plates with borosilicate micropore arrays [6]. In general this type of MCP has performed in accord with the expectations for conventional glass commercial MCPs, with a few exceptions. The borosilicate substrate is more robust than commercial MCPs as has facilitated implementation of MCPs in sizes up to 20 cm, the background rate is intrinsically low, and the ALD provides unique behavior for gain, stability

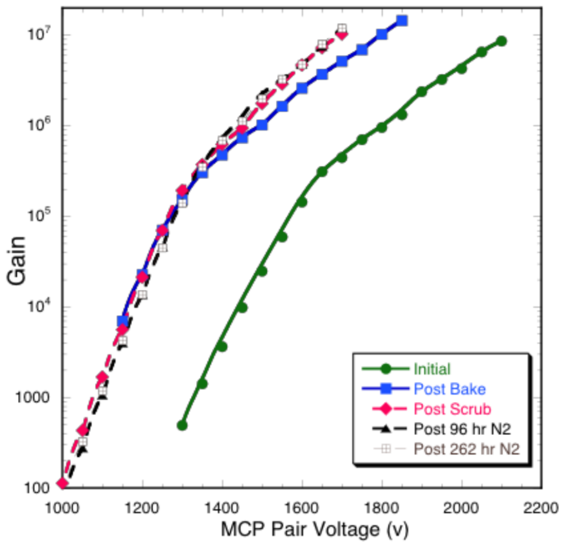

Figure 7. Gain of a pair of 33 mm 20 μm pore, 60 : 1 L/D ALD, borosilicate MCPs during preconditioning steps.

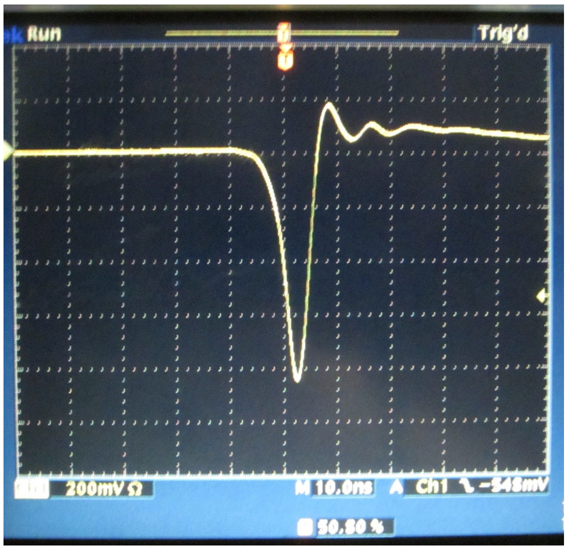

Figure 8. Average single event pulse shape for a 20 cm, MCP pair, 20 μm pore, 60 : 1 L/D, ALD MCPs.

and low outgassing. The main development tool has been 33 mm format size MCPs, but more recently 20 cm square MCPs have been available [6]. The initial gain (figure 7) for 33 mm ALD MCPs is comparable to standard MCPs [1]. However, the MgO ALD layer used as the secondary emissive layer on these MCPs increases its emission coefficient as the surface is cleaned [8] by a high temperature vacuum bake. As a result the gain increases by a factor of 10 or more. Thereafter a standard "burn-in" (scrub) [9] of the MCPs increases the gain only slightly, and the gain remains stable for at least 7 C cm^{-2} of charge extraction. Subsequently, even exposure to dry nitrogen does not modify the gain. Typical pulse risetimes for the 20 μm pore MCP pair configurations are $\sim$ 1 ns [5]. The average pulse shape for amplified event signals detected on the 20 cm detector (figure 2) with a pair of ALD MCPs (20 μm pore, 60 : 1 L/D) and the stripline anode implemented as a serpentine delay line is shown in figure 8. This is largely dominated by the 150 MHz low pass filter in the delay line amplifier chain, but does provide a good signal for timing accuracy (constant fraction discrimination to better than 200 ps) in determination of the event position.

Given the large size of the 20 cm MCPs one concern is the uniformity of the gain and background. Early work [5] showed considerable gain variations spatially. Recent improvements in the ALD deposition technique have resulted in a considerable advance in the uniformity of the gain. Measurements of the MCP performance were made with the open face 20 cm cross delay line detector. Figure 9 shows an enhanced contrast "gain map" image where the color relates to the gain (yellow = high, red = low, average $\sim 5 \times 10^6$). The overall variations of the gain are less than 10% and the granularity is consistent with small gain variations in individual multifiber hexagonal bundles (figure 3). Measurement of the background rate and its uniformity also show improvements due to process development. We find that uniform background rates of $\sim$ 0.055 events cm^{-2} sec^{-1} can be achieved with 20 cm MCP pairs running at $\sim 5 \times 10^6$ gain, with very little "hotspot" activity (figure 10), and pulse amplitude distributions with exponentially dropping

2014 JINST 9 C04002

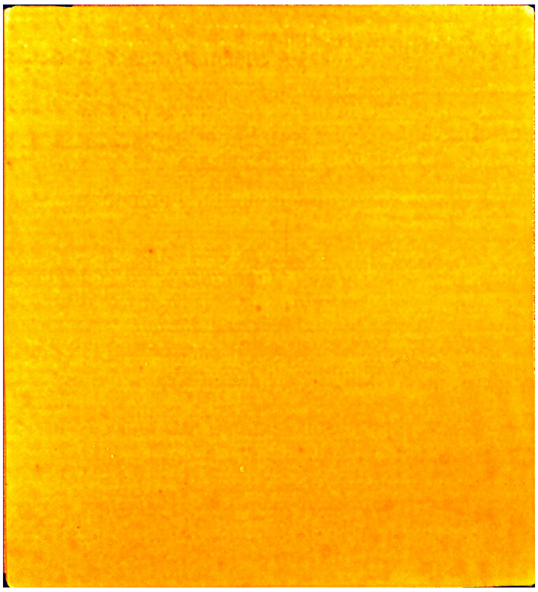

Figure 9. Gain map image for a pair of 20 μm pore, 60 : 1 L/D, ALD borosilicate MCPs, 950v per MCP, 184 nm UV.

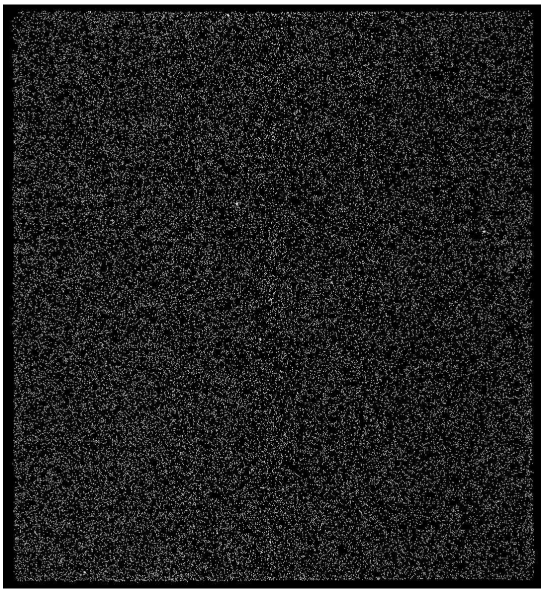

Figure 10. Background event image for a pair of 20 μm pore, 60 : 1 L/D, ALD MCPs. 0.055 events cm^{-2} sec^{-1}.

event rate with increasing amplitude. The intrinsic background rate of MCPs [1] is determined by the residual radioactivity of the MCP glass and by detected cosmic ray Muons. ALD borosilicate glass has a small ^{40}K content ($\sim 4\%$) giving rise to beta decays that are detected. Along with the expected rate of detection of cosmic ray muons (~ 0.02 events cm^{-2} sec^{-1}) this is consistent with our observations of the background rate.

4 20 cm sealed tube results

One of the most challenging issues is the incorporation of large area (20 cm) MCPs into a sealed tube detector (figure 2). One approach we have adopted is to construct a square brazed assembly (figure 2) of kovar and alumina ceramic as the housing for the MCPs. This has a stripline anode and a conventional Indium hot seal well for accomplishing the seal of the window with a bialkali cathode to the detector body.

The detector and MCPs (20 μm pore, 60 : 1 L/D, 8° pore bias, in a chevron pair) were vacuum baked, and the MCPs were subjected to a burn-in before the photocathode was deposited and sealing attempt made. After the bake and burn-in the background of the MCPs was relatively high in several spots (figure 11). This was found to be debris on the MCPs, but did not affect operation in other zones. We have developed a bialkali photocathode deposition technique [10] for large areas using Borofloat 33 substrates that provides a comparatively high quantum efficiency and overall uniformity. In our first sealed tube attempt we achieved a 20 cm bialkali photocathode with a peak efficiency of $\sim 25\%$ (figure 12) and uniformity of $\sim \pm 15\%$. No change in quantum efficiency occurred over a two week period following the cathode deposition.

Immediately after the bialkali photocathode deposition the window was indium sealed to the top of the detector assembly in vacuum and allowed to cool. While still in the vacuum chamber

2014 JINST 9 C04002

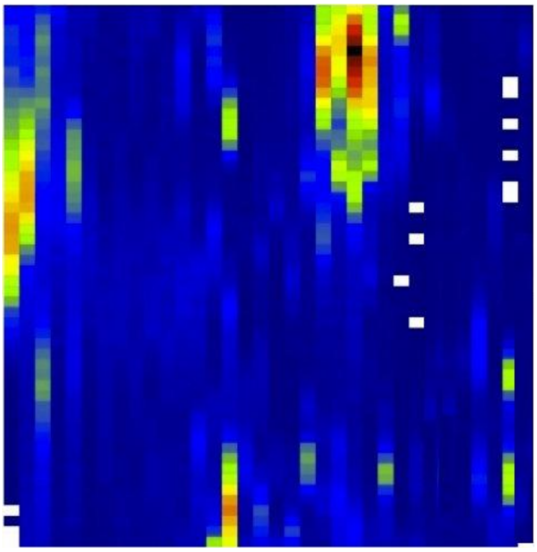

Figure 11. Background event image for a pair of 20 μm pore, 60 :1 L/D, ALD MCPs after processing in a sealed tube (figure 2). $\sim$ 30 kHz rate, mostly in 3 spot areas.

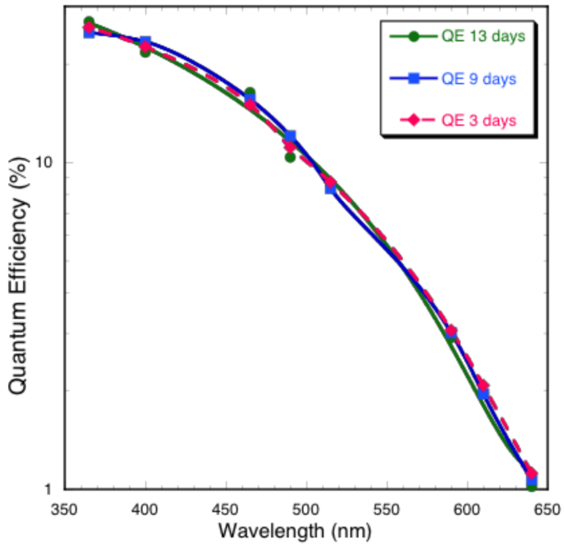

Figure 12. Quantum efficiency for a Na_2KSb bialkali 20×20 cm photocathode on the Borofloat 33 window of a sealed tube test detector (figure 2) for $\sim$ 2 weeks after seal.

a number of evaluation tests on the completed detector were accomplished. Besides the cathode efficiency measurements we also evaluated the imaging using the aforementioned technique of configuring the anode striplines into a delay line readout. Using a 610 nm pulsed (80 ps) laser a spot $\sim$ 5 mm wide was projected into the vacuum tank and onto the photocathode of the sealed detector. Images of that spot were imaged using relatively low MCP gain (5×10^5) but with the laser brightness set to deliver $\sim$ 15 photoelectrons from the photocathode per pulse.

Figure 13 shows the accumulated images of the laser spot projected onto two places on the detector. Due to the coarseness of the anode (5.5 mm strip period) only $\sim 34 \times 50$ electronic pixels can be accommodated, but the spot images show spatial fidelity of $\sim$ 5 mm in X and 7 mm in Y (figure 14). The configuration in the process vacuum tank is not conducive to high quality timing signal propagation, however at $\sim$ 15 photoelectrons per pulse the event timing jitter was measured at $\sim$ 200 ps FWHM using the 80 ps laser pulse. Following testing the completed tube was brought to atmospheric conditions, but unfortunately there was a leak in the indium seal that caused the tube to lose vacuum integrity. This mechanical problem is being resolved for future attempts.

5 10 cm cross strip detector results

To examine the high spatial resolution characteristics of ALD MCPs we installed a pair of 20 μm 60 : 1 L/D, 8° pore bias, as a chevron pair into the 95 mm cross strip detector. This allows high resolution images to be obtained at high counting rates, but at very modest gain levels (10^6) in an event counting mode. Since the image binning is 16k $\times$ 16k (250 Megapixels, at 6 μm) about 10^{10} events were accumulated to see reasonable image statistics. A small section of an image is shown in figure 15, illustrating the hexagonal MCP multifiber structure. The dark hexagon pattern is due to the bottom MCP where low event gain causes events to fall below the electronics threshold. The

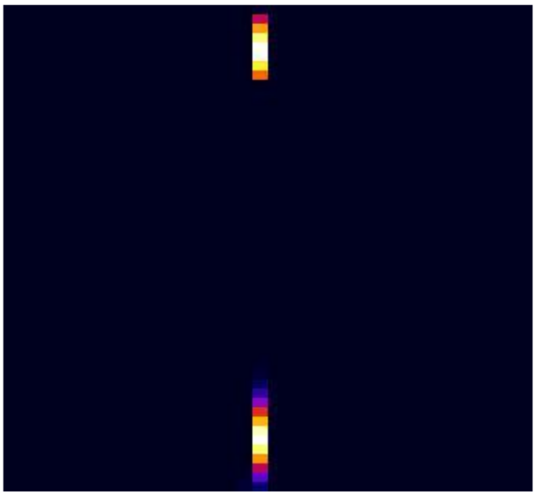

Figure 13. Images of a laser beam ($\sim$ 5 mm spot) in two different positions on the sealed 20 cm test detector (figure 2). 34×50 pixel binning.

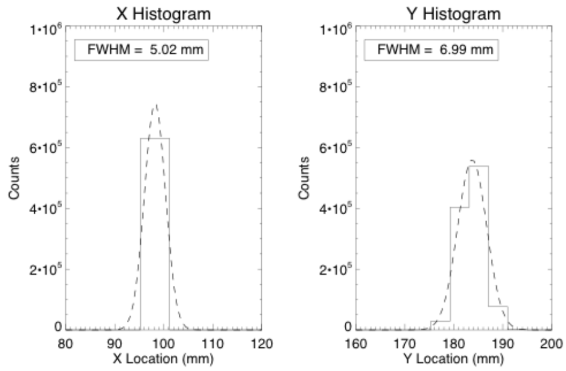

Figure 14. Cross section histograms of the upper spot image in figure 13 showing the imaging of the delay line readout implemented on the stripline readout of the 20 cm sealed tube test detector.

bright/dark hexagon pattern is due to the top MCP where pore crushing at hexagon boundaries causes variation of the detection efficiency for incoming light. Figure 16 shows an expanded area demonstrating the full spatial resolution. This shows that (figure 16, upper) the individual MCP pores (20 μm) can be resolved. The figure 16 lower image that is the map of local gain, shows that all the distorted pores at the hexagonal boundary have lower gain (darker). Those areas with lower gain also have poorer spatial resolution/definition at these reduced signal to noise zones. Significant improvements have been made in the geometrical fidelity of the borosilicate substrates to minimise the hexagonal modulation [5] and those efforts are continuing. With the utilisation of the cross strip detector we can map the electronic effects and correlate them with the geometrical observations by optical microscope to help promote the next iterations of fabrications.

6 Conclusions

Large area detectors employing ALD MCPs on borosilicate substrates have made significant progress in a relatively short period providing large (20 cm) areas, high spatial resolution (20 μm) and time resolution (< 200 ps). The advantages of the ALD MCPs in lifetime stability, robustness, cleanliness and the ability to construct large area formats have significant implications for detectors in both sealed tubes and open face detectors. Applications range from UV imaging and spectroscopy in space based instruments, to high energy physics sensors, detectors for biological imaging/timing, and sensors for ion, or electron spectroscopy and x-ray diffraction. We expect that continuing improvements in substrate fabrication, and ALD layer optimizations will further improve the overall operating fidelity of ALD MCPs. Smaller pore ALD MCPs (10 μm and less) are already under test in large formats (10 cm), and further work in development of sealed tubes is underway.

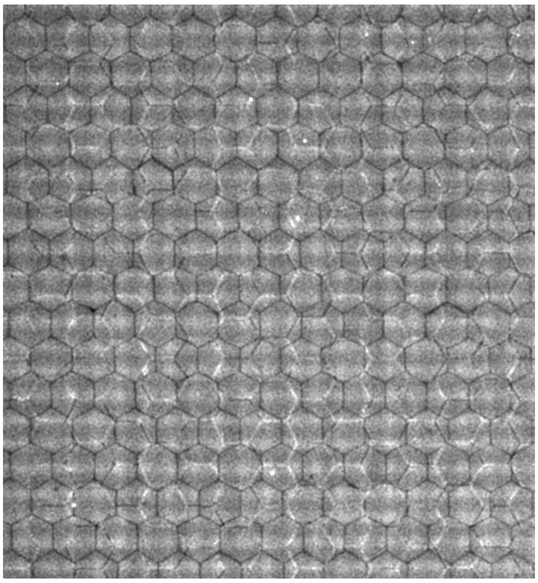

Figure 15. Section (∼ 15 × 15 mm) of an accumulated image for a pair of 20 μm pore 60 :1 L/D ALD MCPs at ∼ 10^6 gain taken with a 95 mm cross strip detector (figure 3), 184 nm UV.

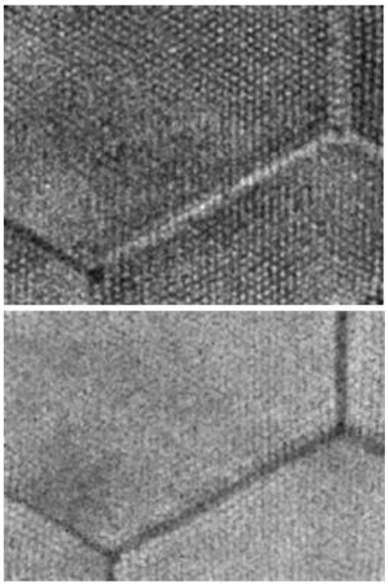

Figure 16. Upper: small image section of figure 15 showing that individual 20 μm MCP pores are resolved. Lower: gain map image of the same area.

Acknowledgments

We acknowledge the efforts of R. Raffanti, J. Hull, S. Jelinsky, J. Tedesco, and our colleagues at Incom Inc. for their assistance in accomplishing these studies. This work was supported by U.S. Department of Energy grant #DE-AC02-06CH11357 and NASA grant NNG11AD54G, and in part by the U.S. Department of Energy under grants DE-SC0009657 and DE-SC0008172.

References

[1] O.H.W. Siegmund, *Methods of vacuum ultraviolet physics*, 2nd edition, J.A.R. Samson and D.L. Ederer eds., Academic Press (1998), chapter III.

[2] M. Lampton, *The microchannel image intensifier*, *Sci. Am.* **245** (1981) 62.

[3] O.H.W. Siegmund et al., *Advances in microchannel plates and photocathodes for ultraviolet photon counting detectors*, *Proc. SPIE* **8145** (2011) 81450J.

[4] A.U. Mane et al., *A novel atomic layer deposition method to fabricate economical and robust large area microchannel plates for photodetectors*, *Phys. Procedia* **37** (2012) 722.

[5] O.H.W. Siegmund et al., *20 cm sealed tube photon counting detectors with novel microchannel plates for imaging and timing applications*, *Phys. Procedia* **37** (2012) 803.

[6] O.H.W. Siegmund et al., *Performance characteristics of atomic layer functionalized microchannel plates*, *Proc. SPIE* **8859** (2013) 88590Y.

[7] O.H.W. Siegmund, J. Vallerga, J. McPhate, B. Welsh and A. Tremsin, *Cross strip readout detectors for high time resolution imaging in the 120 nm to 900 nm wavelength regime*, in Proceedings of the *Advanced Maui Optical and Space Surveillance Technologies Conference*, Wailea Hawaii (2010), pg. E69.

2014 JINST 9 C04002

[8] S.J. Jokela et al., *Secondary electron yield of emissive materials for large-area micro-channel plate detectors: surface composition and film thickness dependencies*, *Phys. Procedia* **37** (2012) 740.

[9] O.H.W. Siegmund, *Preconditioning of microchannel plate stacks*, *Proc. SPIE* **1072** (1989) 111.

[10] O.H.W. Siegmund et al., *Large area and high efficiency photon counting imaging detectors with high time and spatial resolution for night time sensing and astronomy*, in Proceedings of the *Advanced Maui Optical and Space Surveillance Technologies Conference*, Wailea Hawaii (2012).